# = PHYSICS AND TECHNIQUE OF ACCELERATORS

# Longitudinal Dynamic in NICA Barrier Bucket RF System at Transition Energy Including Impedances in BLonD

S. Kolokolchikov<sup>a, b, \*</sup>, Yu. Senichev<sup>a, b</sup>, A. Aksentev<sup>a, b, c</sup>, A. Melnikov<sup>a, b, d</sup>, V. Ladygin<sup>e</sup>, and E. Syresin<sup>e</sup>

<sup>a</sup> Institute for Nuclear Research, Russian Academy of Sciences, Moscow, Russia
 <sup>b</sup> Moscow Institute of Physics and Technology, Dolgoprudny, Russia
 <sup>c</sup> Moscow Engineering Physics Institute, Moscow, Russia
 <sup>d</sup> Landau Institute for Theoretical Physics, Chernogolovka, Russia
 <sup>e</sup> Joint Institute for Nuclear Research, Dubna, Russia
 \*e-mail: sergey.bell13@gmail.com
 Received September 15, 2023; revised November 1, 2023; accepted November 24, 2023

**Abstract**—This paper investigates the influence of space charge impedances, as well as RF resonators, on longitudinal dynamics during transition energy crossing with a jump. One distinctive feature is the use of the Barrier Bucket RF as a result a specific distribution of the beam in the phase space, different from the classical one formed by harmonic RF.

# **DOI:** 10.1134/S1547477124700389

# TRANSITION ENERGY

Considering longitudinal motion, the concept of momentum compaction factor is introduced [1]:

$$\alpha_c = \frac{1}{R_0} \frac{dR}{d\delta} = \alpha_0 + 2\alpha_1 \delta + 3\alpha_2 \delta^2 + \dots \equiv \frac{1}{\gamma_T^2}$$
 (1)

as well as the slip-factor:

$$\eta(\delta) = \eta_0 + \eta_1 \delta + \eta_2 \delta^2 + \cdots, \tag{2}$$

where  $\delta$  is the momentum spread;  $R_0$ , R is the averaged radius of the reference and deviated by  $\delta$  particles;  $\alpha_n$ ,  $\eta_n$  are the nth terms of expansion; and  $\gamma_{tr}$  is transition energy. The coefficients can be related by the rela-

tions  $\eta_0 = \alpha_0 - \frac{1}{\gamma_0^2}$  and  $\eta_1 = \alpha_1 - \frac{\eta_0}{\gamma_0^2} + \frac{3}{2} \frac{\beta^2}{\gamma^2}$ . As can be seen, at a certain energy of the reference particle—transition  $\gamma = \gamma_{tr}$ , the slip-factor takes on a zero value  $\eta = \eta_0 = 0$ .

## TRANSITION ENERGY JUMP

The transition energy jump procedure is used to overcome the transition energy. Thus, it is possible to maintain stable motion of the beam in phase space. This method has been used in many installations and is described in the works [2, 3].

The need for a jump can be understood by considering the dependence on  $\eta(\delta) = \eta_0 + \eta_1 \delta + \cdots$ , equa-

tions of longitudinal motion that describe the evolution of particles in phase space [4]:

$$\frac{d\tau}{dt} = \eta(\delta) \frac{h\Delta E}{\beta^2 E_0}, \quad \frac{d(\Delta E)}{dt} = \frac{V(\tau)}{T_0}.$$
 (3)

During acceleration the slip-factor value  $\eta$ approaches zero for all particles; however, due to the nonzero momentum spread  $\delta$ , term  $\eta_1\delta$  begins to be comparable to  $\eta_0$  and plays an important role on the dynamics near the transition energy. If no measures are taken, then for particles that have overcome the transition energy, the sign of the slip-factor changes. Based on Eqs. (3), it is clear that the motion in the phase plane becomes unstable and leads to loss of the beam. The jump procedure allows, first, during the rise of the transition energy, to keep the beam at a distance sufficient for all particles to have the same sign of the slip-factor. Second, to ensure a rapid transition to a new state, where the slip-factor changes sign, but for all particles it again has the same sign. Stability is ensured by changing the polarity of the holding RF barriers.

The expression for momentum compaction factor can be obtained [5]:

$$\alpha = \frac{1}{C} \int_{0}^{C} \frac{D(s)}{\rho(s)} ds,$$
 (4)

where D(s) is the dispersion function and  $1/\rho(s)$  is the orbital curvature. For a stationary machine, it is possible to vary the dispersion function to change the value

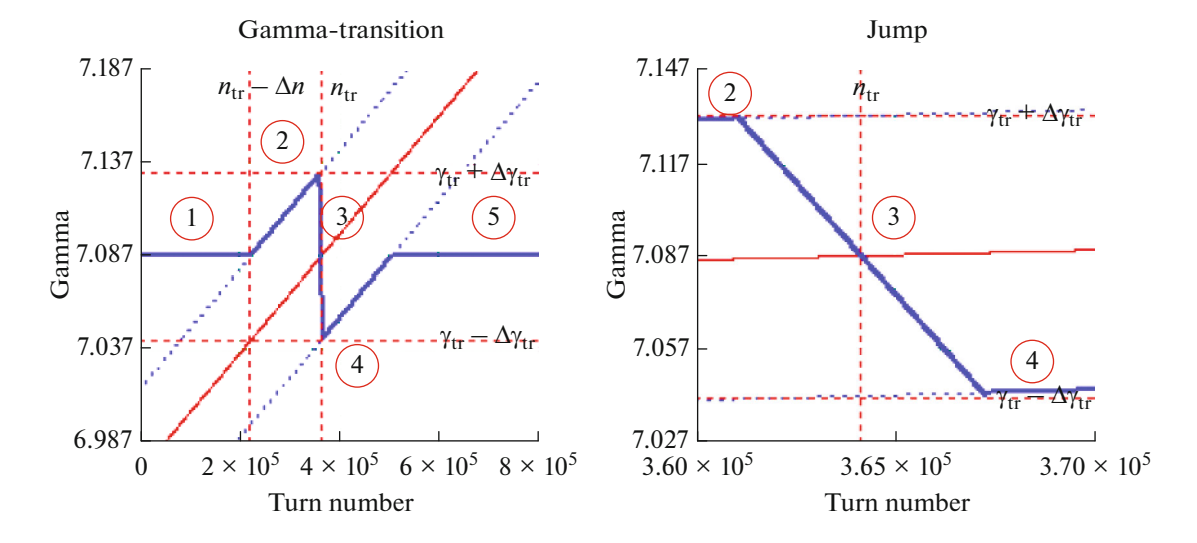


Fig. 1. Scheme of a transition energy jump. The blue line is the actual transition energy of the accelerator  $\gamma_{tr}$ ; the red line is the energy of the reference particle.

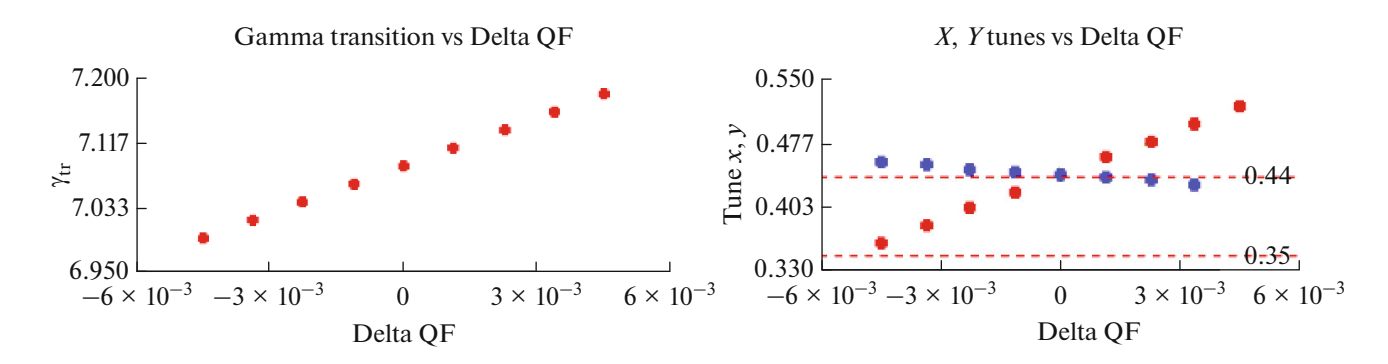


Fig. 2. Dependence of the transition energy and operating point on the perturbation of the gradient of quadrupole lenses.

 $\alpha$  and, accordingly,  $\eta$ . For example, for NICA, the possibility of creating an additional gradient in quadrupole lenses is being considered. Calculations show that it is possible to change the transition energy  $\gamma_{tr}$  with speed  $d\gamma_{tr}/dt = 8.5 \text{ s}^{-1}$  [6].

We can distinguish five main states of longitudinal dynamics based on changes in transition energy  $\gamma_{tr}$  (Fig. 1):

- (1) acceleration from injection energy  $E_{\rm inj}$  with stationary value  $\gamma_{\rm tr}^{\rm stat}$ ;
- (2) smooth increase  $\gamma_{tr}$  parallel to the particle energy up to the peak value and slip-factor  $\eta_0$  acquires the minimum possible value, approaching zero;
- (3) transition through the stationary value of the transition energy, while  $\eta_0$  crosses zero for all particles;

- (4) smooth recovery  $\gamma_{tr}$  to the stationary value, also parallel to the particle energy;
- (5) acceleration to the energy of an experiment with a stationary value of the transition energy  $\gamma_{tr}^{stat}$ .

States 2, 3, and 4 determine the jump procedure for overcoming the  $\gamma_{tr}$ . A change in magneto-optics leads to a dependence  $\gamma_{tr}$  and the corresponding shift of the operating point  $v_{x,y}$  (Fig. 2), as well as higher orders of the momentum compaction factor  $\alpha_1, \alpha_2$  (Fig. 3).

# BARRIER BUCKET RF

To cross transition energy, it is possible to use an RF barrier type (Barrier Bucker RF) [7, 8] (Fig. 4).

$$g(\phi) = \begin{cases} -\operatorname{sgn}(\eta), & -\pi/h_{r} \le \phi \le 0\\ \operatorname{sgn}(\eta), & 0 < \phi \le \pi/h_{r} \end{cases} , \tag{5}$$

$$0, \text{ other}$$

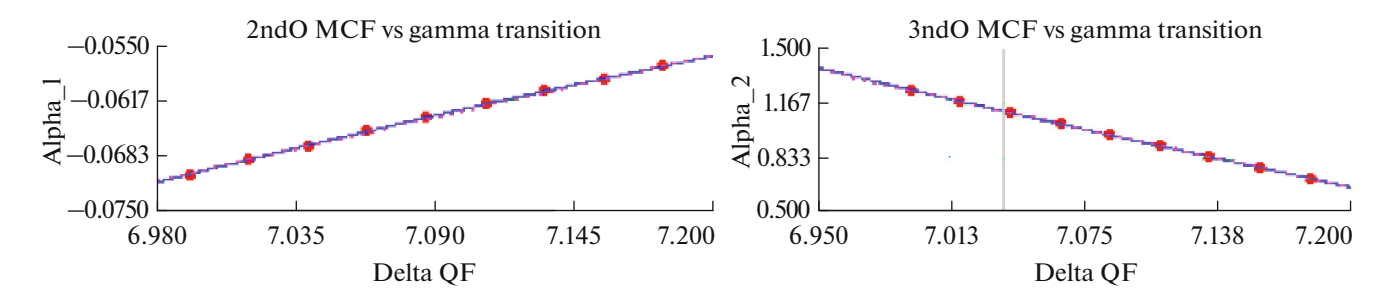


Fig. 3. Dependence of higher orders of expansion of the orbital expansion coefficient on transition energy.

where  $\eta$  is the slip-factor,  $h_{\rm r} = \frac{\pi}{\phi_{\rm r}}$  is the harmonic

number for the reflective barrier, and  $\phi_r$  is the corresponding phase. In Eq. (5), it is taken into account that, when passing through transition energy, the sign  $\eta$  and, accordingly, the polarity of the RF barriers change. For acceleration, additional voltage can also be applied in the form of a meander with voltage  $V_{\rm acc} = 300 \, {\rm eV}$ .

The Fourier expansion coefficients for the reduced square wave signal are given by [9]

$$b_n = \operatorname{sgn}\left(\eta\right) \frac{2}{n\pi} \left[ 1 - \cos\left(\frac{n}{h_r}\pi\right) \right],\tag{6}$$

where n is the harmonic number. To create a smooth signal shape, sigma modulation is used, preserving the symmetry of the signal:

$$\sigma_{m,n} = \operatorname{sinc}^m \frac{n\pi}{2(N+1)},\tag{7}$$

where N is the number of terms of the harmonic expansion. Thus, the voltage of the nth harmonic is

$$V_n = V^{\text{peak}} b_n \sigma_{m,n}. \tag{8}$$

Figure 5 present the resulting waveforms and the corresponding voltages for the harmonics.

Depending on the relative displacement from the reference one, the particles fall under the influence of the RF barrier in the reflection region and experience a push of energy:

$$E_{i}' = \Delta E_{i} + \sum_{i=1}^{N} V_{j} \sin(\omega_{j} \Delta t_{i} + \phi_{j}). \tag{9}$$

# INFLUENCE OF IMPEDANCE

To take into account the influence of the electromagnetic interaction of the beam with its surroundings, the concept of impedance is introduced. The

longitudinal dynamics are mainly influenced by the space charge impedance [10] (Fig. 6):

$$\frac{Z_{\rm SC}}{n} = -\frac{Z_0}{2\beta\gamma^2} \left[ 1 + 2\ln\left(\frac{b}{a}\right) \right]. \tag{10}$$

For clarity, we present the voltage induced by the space charge,  $V_{SC}(\phi)$ . The equation is determined by the derivative of the distribution function  $f(\phi)$  in space [11]:

$$V_{\text{SC}}(\phi) = \frac{Z^2 h^2 g_0 Z_0 ce}{2R_0 \gamma^2} \frac{\partial \left(N_0 f(\phi)\right)}{\partial \phi}.$$
 (11)

For the Barrier Bucket RF, as will be seen further from Figs. 7 and 8, the distribution inside the separatrix is uniform directly outside the reflective barrier. Thus, the derivative differs slightly from zero. Significant induced voltage can only be created at the edges of the separatrix, where a change in the beam profile gradient is observed.

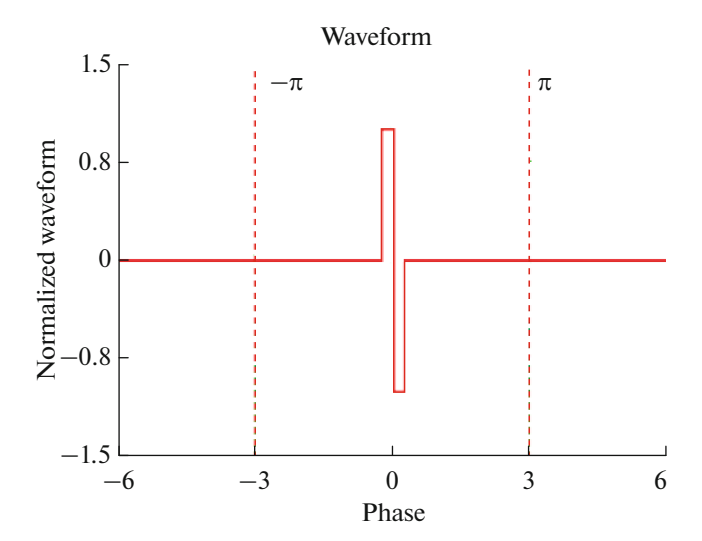
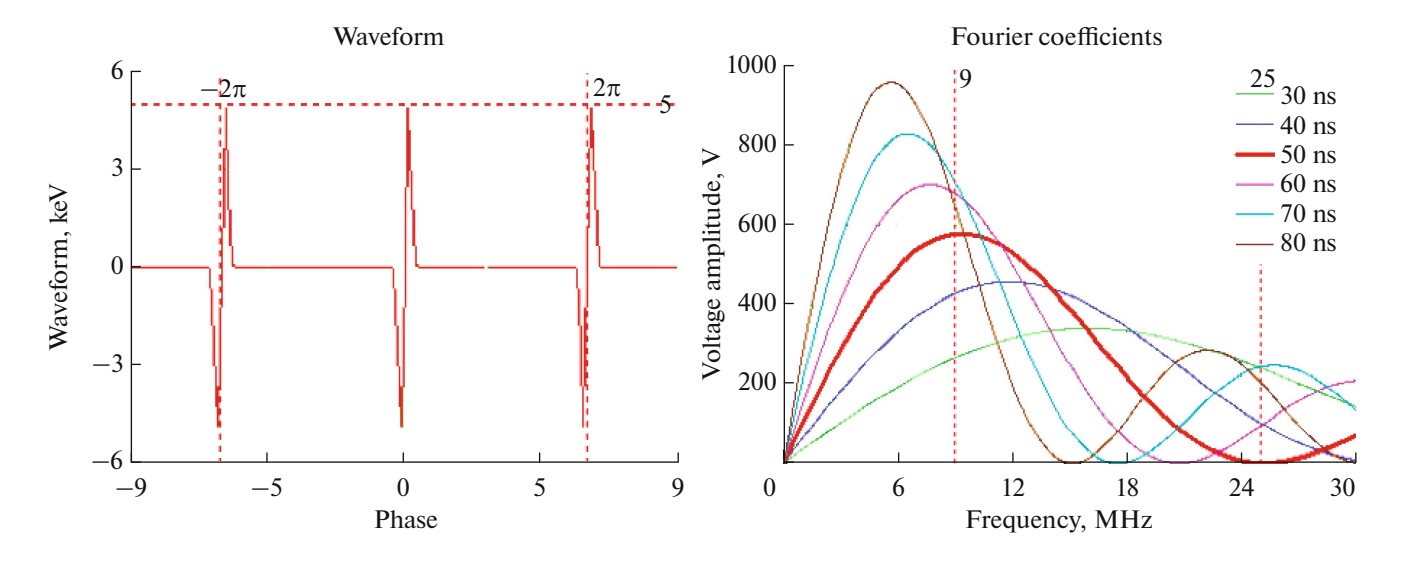


Fig. 4. Normalized waveform from the RF barrier.



**Fig. 5.** Decomposition of a signal from an RF barrier type into a Fourier series in sinusoidal harmonics. On the left is the shape of the Barrier Bucket; on the right are the harmonic amplitudes depending on frequency for different widths of the reflective barrier.

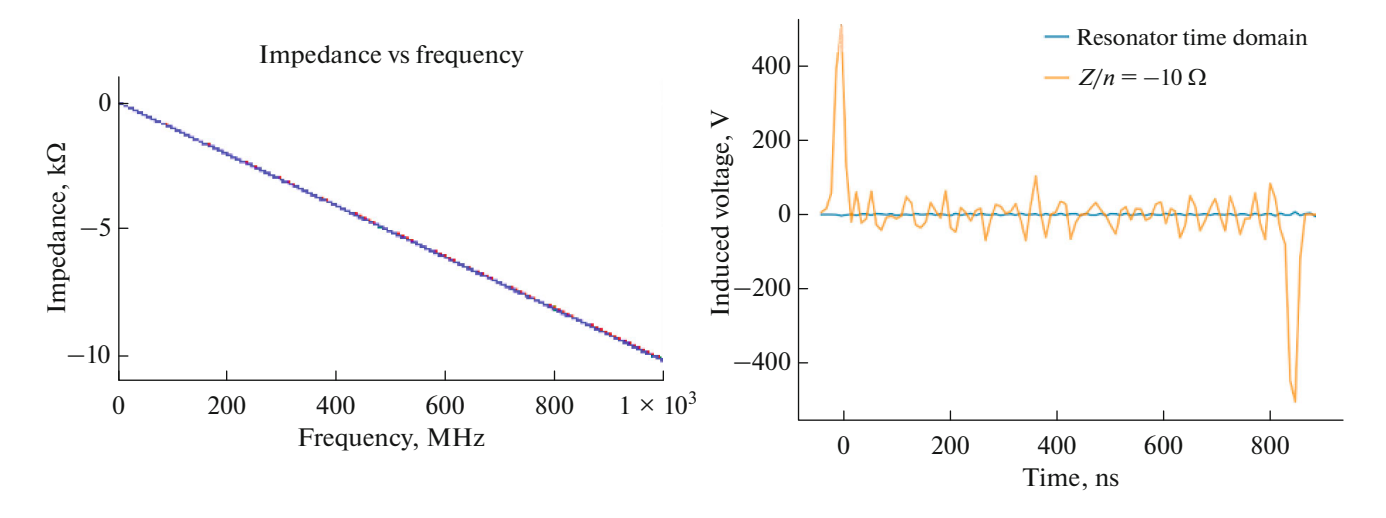


Fig. 6. On the left is the space charge impedance; on the right—induced voltage, created by a space charge along the beam profile in the longitudinal plane.

# **MODELING**

The most dangerous from the point of view of beam destruction are states 2, 3, and 4, in which the accelerator parameters change. From a dynamic point of view, states 2 and 4 are symmetrical.

The beam profile in the longitudinal plane is uniform, and the energy spread is Gaussian. States 2 and 4 are characterized by the fact that the slip-factor for the equilibrium particle remains unchanged, and the transition energy changes synchronously with the beam energy over a period of order  $2 \times 10^5$  turns. Thus, confining the beam at a stationary value of the transition energy is equivalent to the accelerated motion of

the beam in a structure with changing parameters. As can be seen in Fig. 8, the beam profile shifts to the left barrier; this is due to the fact that, for particles with positive  $\delta > 0$ , slip-factor  $\eta_{+\delta}$  is greater than for particles with negative  $\delta < 0$   $\eta_{-\delta}$ :  $\eta_{+\delta} > \eta_{-\delta}$ . This can be seen from Eq. (2) and the fact that  $\eta_1 < 0$ .

State 3 is the rapid change of parameters within  $6 \times 10^3$  turns (10 ms). The Barrier Bucket are turned off for the duration of the jump so as not to destroy the beam. The effect of space charge is the most important in the absence of barriers, since there is no external confining force. Tracking is done taking into account the space charge impedance described above.

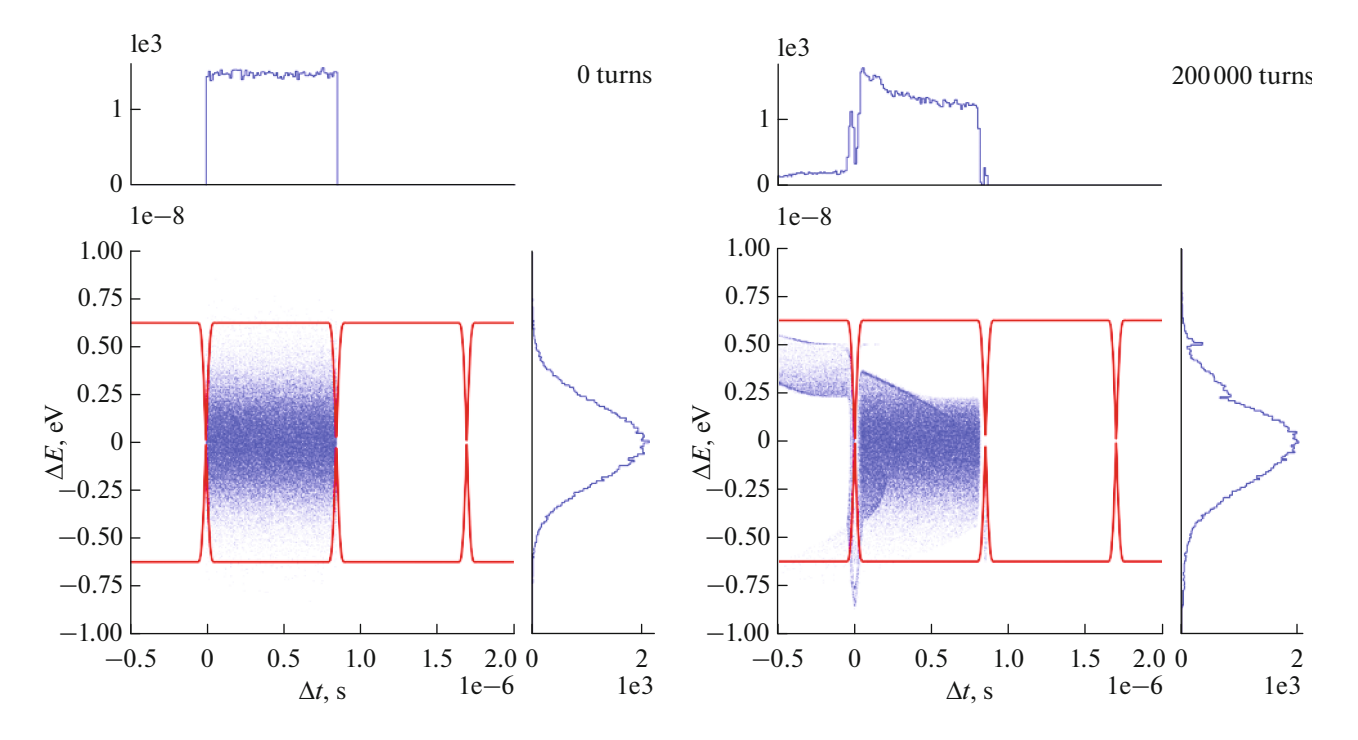


Fig. 7. Phase plane the beam is contained inside Barrier Bucket RF. On the left is the initial distribution, on the right is the distribution after  $2 \times 10^5$  turns.

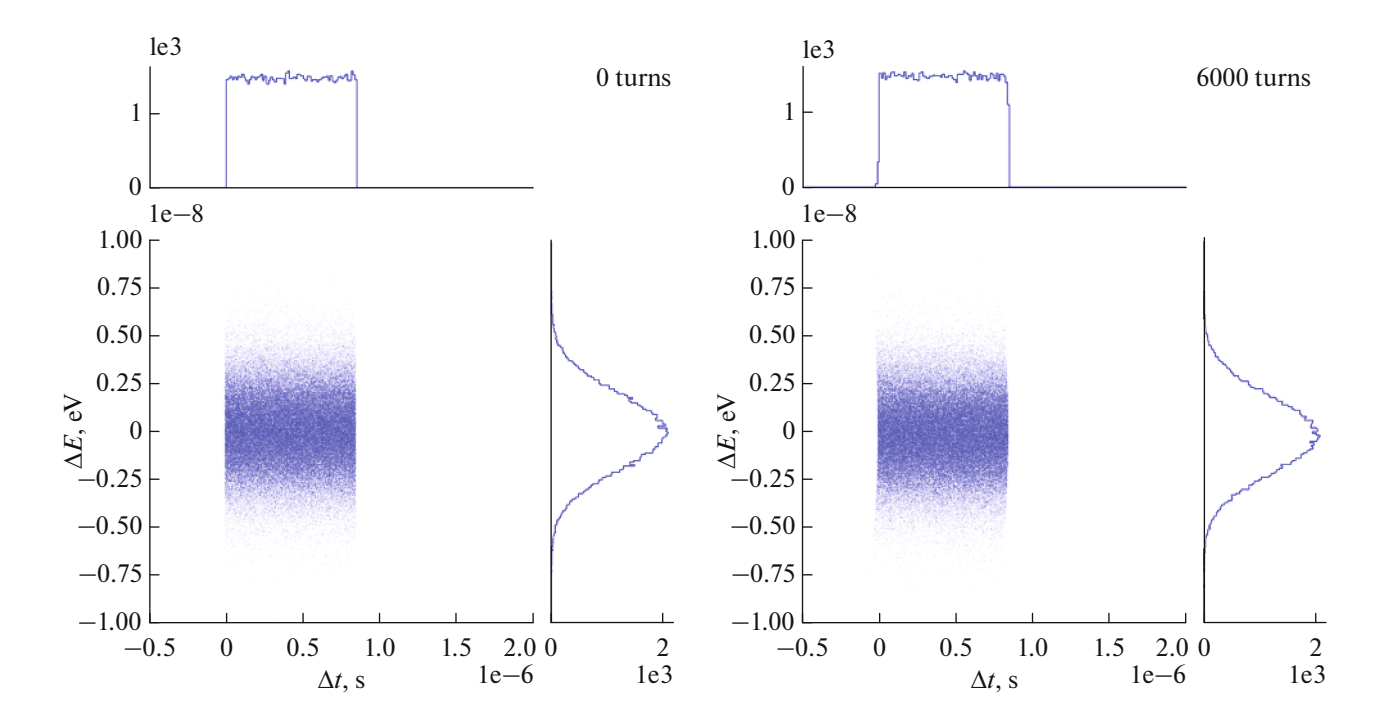


Fig. 8. Phase plane during jump, RF barriers disabled. On the left is the initial distribution, on the right is the distribution after  $6 \times 10^3$  turns.

During the jump, no significant change in the beam profile occurred. Modeling was performed in the BLonD environment [12, 13].

# **CONCLUSIONS**

The dynamics of longitudinal motion near the transition energy in Barrier Bucket RF has been studied, taking into account the space charge impedance. The procedure for rapid changes in accelerator parameters is an accessible option for overcoming the transition energy in barrier RF.

#### **FUNDING**

This research was supported by the Russian Science Foundation no. 22-42-04419 (https://rscf.ru/en/project/22-42-04419/).

## CONFLICT OF INTEREST

The authors of this work declare that they have no conflicts of interest.

## REFERENCES

- S. Y. Lee, *Accelerator Physics*, 3rd ed. (World Scientific, 1998). https://doi.org/10.1142/8335
- T. Risselada, "Gamma transition jump schemes," in Proceedings of CAS-CERN Accelerator School (1994).
- 3. R. Ainsworth at al., "Transition crossing in the main injector for PIP-II," FERMILAB-CONF-17-143-AD.
- Yu. V. Senichev and A. N. Chechenin, Beam Cooling at COSY and HESR.

- Yu. V. Senichev and A. N. Chechenin, "Theory of "resonant" lattices for synchrotrons with negative momentum compaction factor," JETP 105, 988—997 (2007).
- 6. E. M. Syresin at al., "Formation of polarized proton beams in the NICA collider-accelerator complex," Phys. Part. Nucl. **52**, 997—1017 (2021). https://doi.org/10.1134/S1063779621050051
- A. Tribendis at al., "Construction and first test results of the barrier and harmonic RF systems for the NICA collider," in *Proceedings of International Particle Accelerator Conference IPAC2021, Campinas, Brazil, 2021.* https://doi.org/10.18429/JACoW-IPAC2021-MOPAB365
- A. M. Malyshev at al., "Barrier station RF1 of the NICA collider. Design features and influence on beam dynamics," in *Proceedings of Russian Particle Accelera*tor Conference RuPAC2021, Alushta, Russia, 2021. https://doi.org/10.18429/JACoW-RuPAC2021-WEPSC15
- M. Vadai, "Beam loss reduction by barrier buckets in the CERN accelerator complex," (CERN, Geneva, 2021).
- J. L. Laclare, "Coasting beam longitudinal coherent instabilities," in *Proceedings of CAS-CERN Accelerator School: 5th General Accelerator Physics Course*, pp. 349–384. https://doi.org/10.5170/CERN-1994-001.349
- J. Wei and S. Y. Lee, "Space charge effect at transition energy and the transfer of R.F. system at top energy," BNL-41667.
- 12. P. F. Derwent, "Implementation of BLonD for booster simulations," in Beams doc 8690 (2020).
- 13. BLonD https://blond.web.cern.ch/.

**Publisher's Note.** Pleiades Publishing remains neutral with regard to jurisdictional claims in published maps and institutional affiliations.